Local Diagonal Extrema Pattern: A new and Efficient Feature Descriptor for CT Image Retrieval

Shiv Ram Dubey, *Student Member*, *IEEE*, Satish Kumar Singh, *Senior Member*, *IEEE*, and Rajat Kumar Singh, *Member*, *IEEE*

***Abstract*— The medical image retrieval plays an important role in medical diagnosis where a physician can retrieve most similar images from template images against a query image of a particular patient. In this letter, a new and efficient image features descriptor based on the local diagonal extrema pattern (LDEP) is proposed for CT image retrieval. The proposed approach finds the values and indexes of the local diagonal extremas to exploit the relationship among the diagonal neighbors of any center pixel of the image using first-order local diagonal derivatives. The intensity values of the local diagonal extremas are compared with the intensity value of the center pixel to utilize the relationship of central pixel with its neighbors. Finally, the descriptor is formed on the basis of the indexes and comparison of center pixel and local diagonal extremas. The consideration of only diagonal neighbors greatly reduces the dimension of the feature vector which speeds up the image retrieval task and solves the "Curse of dimensionality" problem also. The LDEP is tested for CT image retrieval over Emphysema-CT and NEMA-CT databases and compared with the existing approaches. The superiority in terms of performance and efficiency in terms of speedup of the proposed method are confirmed by the experiments.**

***Index Terms*—Local features, medical image, CT image retrieval, LBP, LTP, LTCoP, local diagonal neighbors.**

I. Introduction

THE research into computer assisted diagnosis using images, signals and videos are an active area nowadays. The X-ray, MRI, CT, etc. is the type of medical images which is mostly accessible to a physician [1]. These images can be processed using pattern recognition and signal analysis tools to extract the information from it [2]. The information contained in the image can be represented in the form of the feature vectors using efficient image descriptors which can be used in the content based image retrieval system to retrieve the most similar images of a given query image [3]-[4]. Content based image retrieval is also applied in medical applications by several researchers [5]-[8].

The performance and time complexity of any image retrieval system is determined by its features extracted [4] [24]. Recently, researchers have used local energy histograms [9], covariate shift methodology [10], shearlet-based energy histograms [11], local contrast pattern [12], Interleaved intensity order based local descriptor [25], etc. to extract the features from the image. Local binary pattern (LBP) is widely adopted feature description method initially introduced for the texture classification by Ojala et al. [13] and has shown very promising results in medical applications also [14]-[16]. The LBP considers a sign of difference of central pixel with its neighbors to describe the local feature of the image. Various variants of the LBP also exist in the literature such as a local ternary pattern (LTP) [17], center symmetric local binary pattern (CSLBP) [18], center symmetric local ternary pattern (CSLTP) [19], data driven local binary pattern (DDLBP) [20], local neighboring intensity relationship pattern (LNIRP) [21], etc. The CSLBP and CSLTP reduce the dimension of the feature vector, but also lost the crucial information which exists between the center pixel and its neighbors. Local mesh pattern (LMeP) [22] and local ternary co-occurrence pattern (LTCoP) [23] are the recent feature description methods introduced by Murala and Wu for the biomedical image retrieval. The LMeP exploits the relationship exists among the local neighboring pixels in various forms, whereas LTCoP is based on the relationship of center pixel with its neighbors and various distances. The main drawback of the LBP, LTP, LMeP and LTCoP is the "curse of dimensionality" with the increasing number of local neighbors. LBP, LTP and LTCoP methods have used only the relationship of central pixel with its neighbors and CSLBP, CSLTP and LMeP methods have used only the relationship between the local neighbors to represent the image.

The high dimensionality and lack of some information of the existing methods are the driving factors for us to propose a new and efficient local feature described in this letter. We used only the center pixel and its local diagonal neighbors to reduce the dimension of the proposed descriptor significantly. Moreover, the number of diagonal neighbors is very limited and doesn't depend upon the radius of local neighborhoods. The information among the local diagonal neighbors is encoded by finding the values and indexes of the local diagonal extremas using first-order local diagonal derivatives. The CSLTP also exploits the local diagonal neighbors, but it doesn't consider the center pixel, whereas we used the relationship of local diagonal extremas with the center pixel to enhance the discriminating ability of the proposed descriptor. The proposed descriptor is tested for CT image retrieval and found the promising performance. The remaining sections of this letter include the computation of proposed descriptor in section 2, CT image retrieval experiments and results in section 3 and concluding remarks in section 4.

II. Local Diagonal Extrema Pattern

In this section, we introduce a new and efficient image feature descriptor using local diagonal extrema pattern (LDEP) from the center pixel and its local diagonal neighbors. The local diagonal extremas (i.e. maxima and minima) are

The authors are with the Indian Institute of Information Technology Allahabad, India (e-mail: shivram1987@gmail.com, sk.singh@iiita.ac.in, rajatsingh@iiita.ac.in).

The final paper is available from http://dx.doi.org/10.1109/LSP.2015.2392623

extracted by using first-order local diagonal derivatives. Further, the relationship of these local diagonal maxima and minima with the center pixel is used to encode the LDEP descriptor.

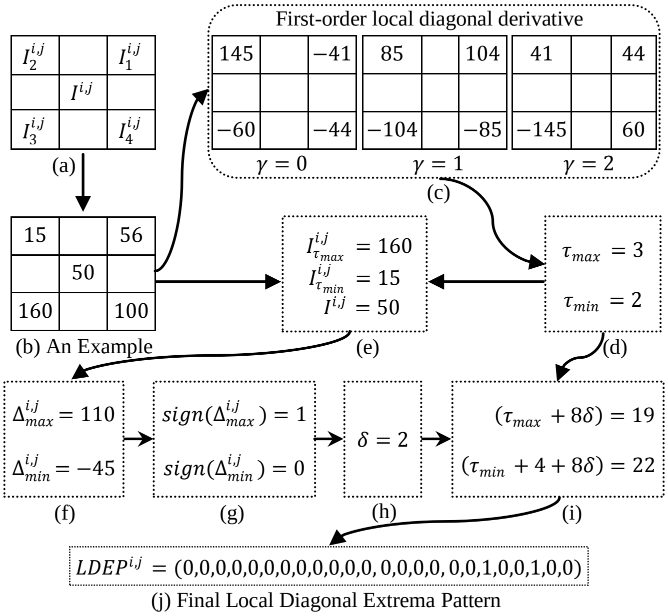

Fig. 1. The computation of $LDEP^{i,j}$ pattern for center pixel $P^{i,j}$ using the flow diagram with an example.

A. First-Order Local Diagonal Derivative

A concept of first-order local diagonal derivative is introduced in this subsection to find the local diagonal maxima and minima (i.e. extremas) of any center pixel. We used only diagonal neighbors because it greatly reduces the dimension of the descriptor and also it is shown that the diagonal neighbors contain most of the local information [19]. Let $P_t^{i,j}$ is the t^{th} diagonal neighbor of any center pixel $P^{i,j}$ at a distance R from the $P^{i,j}$ where $t \in [1,4]$ and $P^{i,j}$ is the pixel at i^{th} row and j^{th} column of any gray scaled image M having m_1 rows and m_2 columns (i.e. the dimension of M is $m_1 \times m_2$). Suppose $I_t^{i,j}$ and $I^{i,j}$ are the intensity values of $P_t^{i,j}$ and $P^{i,j}$ respectively as shown in Fig. 1(a). We defined $I_t^{i,j}$ as follows,

$$I_t^{i,j} = I^{i+\alpha, j+\beta} \tag{1}$$

where α and β are the constants and having the values either $+R$ or $-R$ depending upon the value of t as,

$$\alpha, \beta = \begin{cases} -R, +R & t = 1 \\ -R, -R & t = 2 \\ +R, -R & t = 3 \\ +R, +R & t = 4 \end{cases} \tag{2}$$

We defined three first-order diagonal derivatives for $\gamma = 0, 1$ and 2 respectively. We computed the diagonal derivatives in three directions to encode the relationship of each diagonal with the remaining diagonals in order to find the local diagonal extremas which will be used for finding the relationship with the center pixel.

$$\vec{I}^{i,j}_{t,\gamma} = I^{i,j}_{(1+mod\,(t+\gamma,4))} - I^{i,j}_t \tag{3}$$

where $t \in [1,4]$, $\gamma \in [0,2]$ and $mod(\lambda_1, \lambda_2)$ is the reminder of division of λ_1 by λ_2. Fig. 1(c) depicts the first-order diagonal derivatives for $\gamma = 0, 1$ and 2 computed over an example of Fig. 1(b). The local diagonal maxima and local diagonal minima of the center pixel $P^{i,j}$ are represented by $P^{i,j}_{\tau_{max}}$ having intensity value $I^{i,j}_{\tau_{max}}$ and $P^{i,j}_{\tau_{min}}$ having an intensity value $I^{i,j}_{\tau_{min}}$ respectively, where τ_{max} and τ_{min} are the indexes of the local diagonal maxima and local diagonal minima of $P^{i,j}$ respectively and defined as follows,

$$\tau_{max} = \underset{t}{argmax}\left(sign\left(\vec{I}^{i,j}_{t,\gamma}\right) = 0, \quad \forall\, \gamma \in [0,2]\right) \tag{4}$$

$$\tau_{min} = \underset{t}{argmin}\left(sign\left(\vec{I}^{i,j}_{t,\gamma}\right) = 1, \quad \forall\, \gamma \in [0,2]\right) \tag{5}$$

where $sign$ is a function to find the sign of a number and defined as follows,

$$sign(\lambda) = \begin{cases} 1, & \lambda \geq 0 \\ 0, & \lambda < 0 \end{cases} \tag{6}$$

Now after performing first-order diagonal derivatives, we computed the values and indexes of the local diagonal extremas which will be used with the central pixel to form the local diagonal extrema pattern. Fig. 1(d) displayed the indexes of the local diagonal extremas computed from Fig. 1(c) (i.e. first-order local diagonal derivatives). Fig. 1(e) shows the values of the local diagonal extremas and center pixel.

B. Local Diagonal Extrema Pattern

For the central pixel $P^{i,j}$ having intensity value $I^{i,j}$, τ_{max} and τ_{min} are the indexes and $I^{i,j}_{\tau_{max}}$ and $I^{i,j}_{\tau_{min}}$ are the values of the local diagonal maxima and local diagonal minima respectively. We represent the local diagonal extrema pattern (LDEP) for $P^{i,j}$ with a binary pattern $LDEP^{i,j}$ when the local diagonal neighbors at a distance R are considered and generated as follows,

$$LDEP^{i,j} = \left(LDEP_1^{i,j}, LDEP_2^{i,j}, \ldots, LDEP_{dim}^{i,j}\right) \tag{7}$$

where dim is the length of the $LDEP$ pattern and $LDEP_k^{i,j}$ is the k^{th} element of the $LDEP^{i,j}$ and given using following formulae,

$$LDEP_k^{i,j} = \begin{cases} 1, & if\ k = (\tau_{max} + 8\delta)\ or\ k = (\tau_{min} + 4 + 8\delta) \\ 0, & Else \end{cases} \tag{8}$$

where δ is a variable to denote the extrema-center relationship factor. The $LDEP^{i,j}$ pattern is all 0's with two 1's and the positions of the 1's are determined on the basis of the indices of the extremas and the relationship of the extremas with the center pixel (i.e. τ_{max}, τ_{min} and δ). The extrema-center relationship factor quantifies the relationship of center with the extremas and defined as,

$$\delta = \begin{cases} 0, & If\ \left(sign\left(\Delta^{i,j}_{max}\right) = 0\ and\ sign\left(\Delta^{i,j}_{min}\right) = 0\right) \\ 1, & If\ \left(sign\left(\Delta^{i,j}_{max}\right) = 1\ and\ sign\left(\Delta^{i,j}_{min}\right) = 1\right) \\ 2, & Else \end{cases} \tag{9}$$

where $sign$ is defined in (6) and $\Delta^{i,j}_{max}$ and $\Delta^{i,j}_{min}$ are the local diagonal extrema-center difference factor for $I^{i,j}_{\tau_{max}}$ and $I^{i,j}_{\tau_{min}}$ respectively and computed as follows,

$$\Delta^{i,j}_{max} = I^{i,j}_{\tau_{max}} - I^{i,j} \tag{10}$$

$$\Delta^{i,j}_{min} = I^{i,j}_{\tau_{min}} - I^{i,j} \tag{11}$$

Note that the dimension of the pattern $LDEP^{i,j}$ is the maximum possible value of k which in turns depends upon the maximum possible values of τ_{min} and δ. When $\tau_{min} = 4$ and $\delta = 2$, then the maximum possible value of k is 24, it means that the dimension dim of the $LDEP^{i,j}$ is 24. The low dimension of the proposed pattern is the main benefit of our method. Fig. 1(f-g) shows the difference and sign of difference of local diagonal extremas with the center pixel of example of Fig. 1(b). The value of δ for this example is demonstrated in the Fig. 1(h) and Fig. 1(i) shows the values of $(\tau_{max} + 8\delta)$ and $(\tau_{min} + 4 + 8\delta)$. Finally, the LDEP pattern is depicted in Fig. 1(j) for this example. Only two elements of the pattern are set to 1 and the rest are zeros.

The computed local diagonal extrema pattern for the pixel $P^{i,j}$ is $LDEP^{i,j}$. The local diagonal extrema pattern (LDEP) over the image M is given as follows,

$$LDEP = (LDEP_1, LDEP_2, \ldots, LDEP_{dim}) \tag{12}$$

where $LDEP_k$ is the k^{th} element of $LDEP$ and given as follows,

$$LDEP_k = \frac{1}{(m_1 - 2R)(m_2 - 2R)} \sum_{i=R+1}^{m_1-R} \sum_{j=R+1}^{m_2-R} LDEP_k^{i,j} \tag{13}$$

III. Experiments and Results

In this letter, an efficient local diagonal extrema pattern based image descriptor is proposed. The proposed LDEP (dim: 24) descriptor is used in the medical image retrieval experiments to test its discriminative ability and efficiency. We performed the experiments over two medical image databases. The proposed method is compared with LBP (dim: 256) [13], LTP (dim: 2×256) [17], CSLBP (dim: 16) [18], CSLTP (dim: 9) [19], LMeP (dim: 3×256) [22] and LTCoP (dim: 2×256) [23] descriptors because these methods also encode the local neighboring information. The value of R is set to one in the experiments of this letter.

We adopted same similarity measure and evaluation criteria as used in [22]-[23]. The d_1 distance based similarity measure is used in the experiments to find the similarity between the feature vectors of two images and defined as,

$$d_1(q, db) = \sum_{\lambda=1}^{dim} \left| \frac{\mathcal{H}^{db_\omega}(\lambda) - \mathcal{H}^q(\lambda)}{1 + \mathcal{H}^{db_\omega}(\lambda) + \mathcal{H}^q(\lambda)} \right| \tag{14}$$

where dim is the dimension of the feature descriptor, $\mathcal{H}^q(\lambda)$ is the λ^{th} element of the feature descriptor of the query image and $\mathcal{H}^{db_\omega}(\lambda)$ is the λ^{th} element of the feature descriptor of ω^{th} image of the database db.

The experimental results are represented using average retrieval precision (ARP), average retrieval rate (ARR) and F_score as the functions of the number of top matches (η) as,

$$ARP = \frac{100}{\Lambda} \sum_{\omega=1}^{\Lambda} \frac{r(db_\omega)}{\eta} \tag{15}$$

$$ARR = \frac{100}{\Lambda} \sum_{\omega=1}^{\Lambda} \frac{r(db_\omega)}{g(db_\omega)} \tag{16}$$

$$F\_score = \frac{2 \times ARP \times ARR}{ARP + ARR} \tag{17}$$

where Λ is the total number of images in the database db, $r(db_\omega)$ and $g(db_\omega)$ are the number of relevant retrieved images and the number of relevant ground truth images for the ω^{th} query image of db.

In this letter, all the experiments are carried out using a computer having Intel(R) Core(TM) i5 CPU 650@3.20 GHz processor, 4 GB RAM, and 32-bit Windows-7-Ultimate operating system. In this section, first we present the experimental results and discussions over two medical image databases: 1) Emphysema-CT Database and 2) NEMA-CT database. The CT images are having the following two major advantages: first, the superimposition of images of structures outside the area of interest is completely eliminated; second, the tissues that differ in physical density by less than 1% can be distinguished easily because of the inherent high-contrast resolution of CT images.

A. Results over Emphysema-CT Database

Emphysema is characterized by loss of lung tissue and the recognition of emphysematous and healthy lung tissue is useful for a more detailed analysis of the disease. The Emphysema-CT database contains three categories including Normal Tissue (NT), Centrilobular Emphysema (CLE), and Paraseptal Emphysema (PSE) containing 59, 50 and 59 images respectively collected from 39 subjects [26].

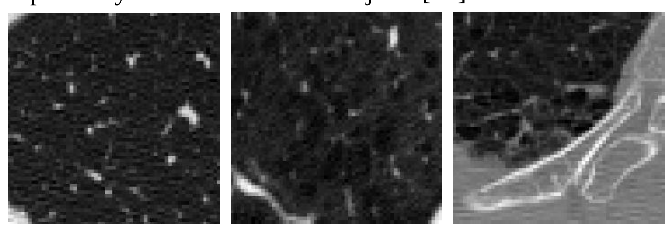

Fig. 2. One sample image from each category of the Emphysema-CT database.

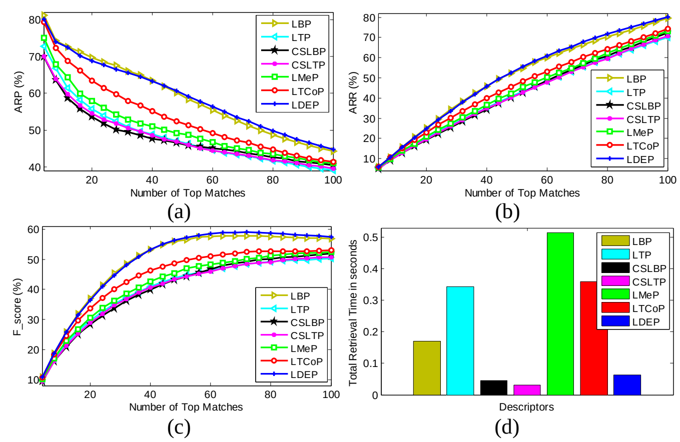

Fig. 3. Comparison of the (a) ARP (%) vs η, (b) ARR (%) vs η, (c) F_score (%) vs η and (d) total retrieval time in seconds using LBP, LTP, CSLBP, CSLTP, LMeP, LTCoP and LDEP descriptors over Emphysema-CT database.

Table 1. The values of the ARP, ARR and F_score using each descriptor over Emphysema database for $\eta = 100$

Performance	Method						
	LBP	LTP	CSLBP	CSLTP	LMeP	LTCoP	LDEP
ARP (%)	44.31	39.15	40.46	39.60	40.99	41.36	44.74
ARR (%)	79.56	70.19	72.31	70.62	73.28	74.30	80.27
F_score (%)	56.92	50.26	51.89	50.75	52.58	53.14	57.46

We characterized the emphysema morphology by describing the Emphysema-CT image intensity patterns using texture analysis techniques and analyzed the performance by retrieving the similar images against each image of the database. Fig. 2 exhibits one sample image from each category of the Emphysema-CT database. The ARP (%), ARR (%) and F_score (%) obtained over Emphysema-CT database for different number of top matches (η) using LBP, LTP, CSLBP, CSLTP, LMeP, LTCoP and LDEP descriptors are compared in the Fig. 3(a-c) respectively. In table 1, these values are summarized for $\eta = 100$. Each of ARP, ARR and F_score is either better or nearly equal using the proposed descriptor as compared to the other descriptors. The total retrieval time is also depicted for each descriptor in Fig. 3(d) in seconds. The retrieval using LDEP is 2.71, 5.46, 8.16 and 5.70 times faster than LBP, LTP, LMeP and LTCoP respectively. From the results of the Fig. 3 and Table 1, it is confirmed that the proposed descriptor is superior as compared to the other descriptors over Emphysema-CT database.

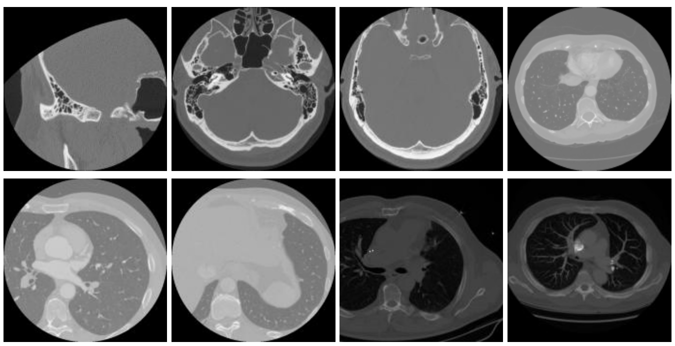

Fig. 4. The example images from the NEMA-CT database, one image from each group.

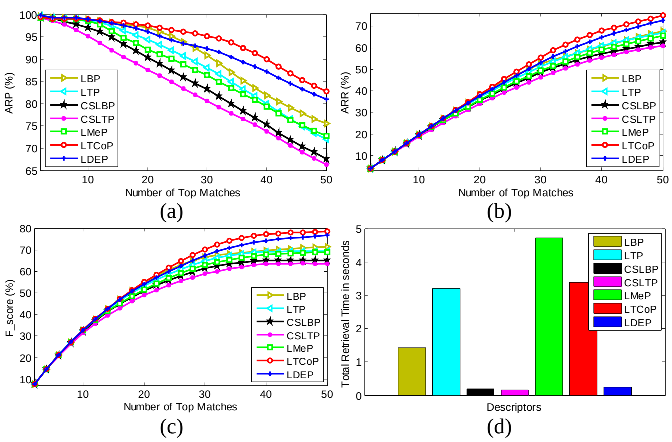

Fig. 5. Comparison of the (a) ARP (%) vs η, (b) ARR (%) vs η, (c) F_score (%) vs η and (d) total retrieval time in seconds using each descriptor over NEMA-CT database.

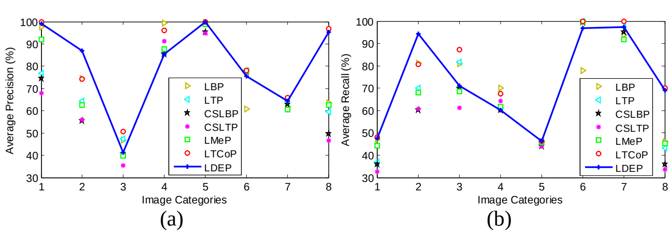

Fig. 6. A categorical performance comparison of each descriptor using (a) average precision and (b) average recall over NEMA-CT database for $\eta = 50$.

B. Results over NEMA-CT Database

The digital imaging and communications in medicine (DICOM) standard are created by the National Electrical Manufacturers Association (NEMA) [27] in order to assist the storage and uses of medical images for research and diagnosis purpose. We considered the CT0001, CT0003, CT0020, CT0057, CT0060, CT0080, CT0082, and CT0083 cases of this database in this paper. We collected 499 CT images (dimension: 512×512) of different parts of the body from the NEMA database in this experiment and categorized it into 8 categories having 104, 46, 29, 71, 108, 39, 33 and 69 images to form the NEMA-CT database. Fig. 4 shows one sample image from each category of this database.

We have illustrated the results compared among each descriptor over NEMA-CT database in terms of the ARP, ARR and F_score by varying the number of top matches in the Fig. 5(a-c) respectively. The total retrieval time in seconds is also depicted for each descriptor in Fig. 5(d). It is evident that the performance of LDEP is better as compared to other descriptors except LTCoP over NEMA-CT database. Moreover, the performance of LDEP is nearly equal to the LTCoP but the retrieval time using LDEP is 13.54 times faster than LTCoP. To know the retrieval performance of each descriptor over each category of the NEMA-CT database, we have shown the results in terms of the average precision and average recall over each category in the Fig. 6(a-b) respectively. The performance of LDEP is better in most of the categories of the NEMA-CT database.

From the retrieval experiments over Emphysema-CT and NEMA-CT database, it is deduced that the LDEP descriptor is the most discriminating descriptor among the computationally efficient ones. In the emphysema CT data set, our proposed texture descriptor is effectively distinguishing normal lung tissue from 2 different disease cases, and in the NEMA-CT data set, our descriptor is helping to decide which axial section a given input CT slice belongs to.

IV. Conclusion

In this letter, we presented an efficient image feature descriptor for CT image retrieval by exploring the local diagonal extrema pattern (LDEP). To this end, the values and indexes of the local diagonal extremas are computed by applying first-order local diagonal derivatives. Then, these extremas are compared with the center pixel to find the local diagonal neighbor-center relationship factor which is used with the indexes of the local diagonal extremas to form the proposed descriptor. The LDEP encodes the relationship between neighbors as well as center pixel and its neighbors. The resulting descriptor is compact, discriminative as well as efficient. Moreover, the dimension of the proposed descriptor is not affected by any parameter. Extensive experiments over two CT image databases confirmed the superiority of our descriptor for efficient CT image retrieval task.

References

[1] D. L. Rubin, H. Greenspan, and J. F. Brinkley, “Biomedical Imaging Informatics,” *Biomedical Informatics*, pp. 285-327, 2014. Springer London.

[2] A. Meyer-Baese and V.J. Schmid, "*Pattern Recognition and Signal Analysis in Medical Imaging*," 2nd Ed., Elsevier, 2014.

[3] A.W.M. Smeulders, M. Worring, S. Santini, A. Gupta, and R. Jain, "Content-based image retrieval at the end of the early years," *IEEE Trans. Pattern Anal. Mach. Intell.*, vol. 22, no. 12, pp. 1349–1380, Dec. 2000.

[4] Y. Liu, D. Zhang, G. Lu, and W. Y. Ma, "A survey of content-based image retrieval with high-level semantics," *Pattern Recog.*, vol. 40, pp. 262–282, 2007.

[5] H. Muller, A. Rosset, J. P. Vallee, and A. Geisbuhler, "Comparing feature sets for content-based image retrieval in a medical case database," in *Proc. SPIE Med. Imag., PACS Imag. Inf.*, 2004, pp. 99 - 109.

[6] H. Muller, N. Michoux, D. Bandon, and A. Geisbuhler, "A review of content-based image retrieval systems in medical applications - Clinical benefits and future directions," *J. Med. Inf.*, vol. 73, no. 1, pp. 1-23, 2004.

[7] G. Quellec, M. Lamard, G. Cazuguel, B. Cochener, and C. Roux, "Wavelet optimization for content-based image retrieval in medical databases," *J. Med. Image Anal.*, vol. 14, pp. 227-241, 2010.

[8] J. C. Felipe, A. J. M. Traina, and C. Traina Jr., "Retrieval by content of medical images using texture for tissue identification," in *Proc. 16th IEEE Symp. Comput.-Based Med. Syst.*, 2003, pp. 175-180.

[9] Y. Dong, and J. Ma, "Wavelet-based image texture classification using local energy histograms," *IEEE Signal Processing Letters*, vol. 18, no. 4, pp. 247-250, 2011.

[10] A. Hassan, F. Riaz, and A. Shaukat, "Scale and Rotation Invariant Texture Classification Using Covariate Shift Methodology," *IEEE Signal Processing Letters*, vol. 21, pp. 321-324, 2014.

[11] J. He, H. Ji, and X. Yang, "Rotation invariant texture descriptor using local shearlet-based energy histograms," *IEEE Signal Processing Letters*, vol. 20, no. 9, pp. 905-908, 2013.

[12] T. Song, H. Li, F. Meng, Q. Wu, B. Luo, B. Zeng, and M. Gabbouj, "Noise-Robust Texture Description Using Local Contrast Patterns via Global Measures," *IEEE Signal Processing Letters*, vol. 21, no. 1, pp. 93-96, 2014.

[13] T. Ojala, M. Pietikainen, and T. Maenpaa, "Multiresolution gray-scale and rotation invariant texture classification with local binary patterns," *IEEE Trans. Pattern Anal. Mach. Intell.*, vol. 24, no. 7, pp. 971-987, 2002.

[14] S. He, J. J. Soraghan, B. F. O'Reilly, and D. Xing, "Quantitative analysis of facial paralysis using local binary patterns in biomedical videos," *IEEE Trans. Biomed. Eng.*, vol. 56, no. 7, pp. 1864-1870, 2009.

[15] L. Sorensen, S. B. Shaker, and M. de Bruijne, "Quantitative analysis of pulmonary emphysema using local binary patterns," *IEEE Trans. Med. Imag.*, vol. 29, no. 2, pp. 559-569, 2010.

[16] S. Peng, D. Kim, S. Lee, and M. Lim, "Texture feature extraction on uniformity estimation for local brightness and structure in chest CT images," *J. Compt. Biol. Med.*, vol. 40, pp. 931-942, 2010.

[17] X. Tan and B. Triggs, "Enhanced local texture feature sets for face recognition under difficult lighting conditions," *IEEE Trans. Image Process.*, vol. 19, no. 6, pp. 1635-1650, 2010.

[18] M. Heikkil, M. Pietikainen, and C. Schmid, "Description of interest regions with local binary patterns," *Pattern Recog.*, vol. 42, pp. 425-436, 2009.

[19] R. Gupta, H. Patil, and A. Mittal, "Robust order-based methods for feature description," In *the Proceedings of the IEEE International Conference on Computer Vision and Pattern Recognition*, 2010, pp. 334-341.

[20] J. Ren, X. Jiang, J. Yuan, and G. Wang, "Optimizing LBP Structure For Visual Recognition Using Binary Quadratic Programming," *IEEE Signal Processing Letters*, vol. 21, no. 11, pp. 1346-1350, 2014.

[21] K. Wang, C-E. Bichot, C. Zhu, and B. Li, "Pixel to Patch Sampling Structure and Local Neighboring Intensity Relationship Patterns for Texture Classification," *IEEE Signal Processing Letters*, vol. 20, no. 9, pp. 853-856, 2013.

[22] S. Murala and Q. M. J. Wu, "Local Mesh Patterns Versus Local Binary Patterns: Biomedical Image Indexing and Retrieval," *IEEE Journal of Biomedical and Health Informatics*, vol.18, no.3, pp. 929-938, 2014.

[23] S. Murala and Q. M. J. Wu, "Local ternary co-occurrence patterns: A new feature descriptor for MRI and CT image retrieval," *Neurocomputing*, vol. 119, pp. 399-412, 2013.

[24] S. R. Dubey, S. K. Singh, and R. K. Singh, "A multi-channel based illumination compensation mechanism for brightness invariant image retrieval," *Multimedia Tools and Applications*, 2014. DOI: 10.1007/s11042-014-2226-5

[25] S. R. Dubey, S. K. Singh, and R. K. Singh, "Rotation and Illumination Invariant Interleaved Intensity Order Based Local Descriptor," *IEEE Transactions on Image Processing*, vol. 23, no. 12, pp. 5323-5333, 2014.

[26] L. Sørensen, S. B. Shaker, and M. de Bruijne, "Quantitative Analysis of Pulmonary Emphysema using Local Binary Patterns," *IEEE Transactions on Medical Imaging*, vol. 29, no. 2, pp. 559-569, 2010.

[27] NEMA–CT image database, Available from [Online]: ⟨ftp://medical.nema.org/ medical/Dicom/Multiframe/⟩.